Production of Submicron Diameter Silk Fibers under Benign Processing Conditions by Two-Fluid Electrospinning

Mao Wang,[†] Jian H. Yu,[†] David L. Kaplan,[‡] and Gregory C. Rutledge*,[†]

Department of Chemical Engineering and Institute for Soldier Nanotechnologies, Massachusetts Institute of Technology, Cambridge, Massachusetts 02139, and Department of Chemical and Biological Engineering, Tufts University, Medford, Massachusetts 02155

Received August 10, 2005; Revised Manuscript Received November 1, 2005

ABSTRACT: An environmentally benign, entirely aqueous process is described to produce solid, crystallized silk fibers with diameters that are much smaller than natural silk fibers. The process entails three steps. First, submicron diameter fibers with a coaxial internal structure consisting of a silk core and poly(ethylene oxide) (PEO) shell are produced by a two-fluid electrospinning technique at ambient conditions using water as the common solvent. The two-fluid electrospinning process is the key to produce a continuous core filament of unblended silk. No significant mixing between the two fluids was observed to occur during electrospinning. Second, the silk/PEO fibers are annealed under high humidity to induce the conformation transformation from the random coil and/or silk I to predominantly β sheet (silk II) structure. The large surface area of the submicron diameter fibers and the molecular orientation of silk fibroins obtained through electrospinning are believed to facilitate the conformational transformation. Finally, the PEO shell is extracted with water from the now insoluble silk core filament, resulting in a solid, crystallized silk fiber with diameter as small as 170 nm.

Introduction

Silk fibroin has been widely investigated as a biomaterial for applications such as medical sutures and tissue engineering scaffolds due to its excellent biocompatibility, biodegradability, and mechanical properties.[1−4] Recently, there has been renewed interest in the use of natural fibers, particularly those that are environmentally benign, for commercial applications such as medical sutures, drug delivery, tissue scaffolds, and wound dressings.[1,5] Recent advances in molecular biotechnology and protein engineering offer the capability to produce large quantities of silk and other polypeptide-based biopolymers.[2,5,6] However, there remains to date no commercially feasible method for manufacturing synthetic fibers from such biopolymers such that they retain the excellent intrinsic properties, such as biocompatibility and mechanical properties, of natural silk fibers.

A wet spinning technique was first invented by Dupont[7,8] in the early 1990s and then developed by others to spin artificial silk protein fibers with diameter in the range of tens of microns.[9−13] Recently, electrospinning has been used to produce submicron diameter artificial silk fibers.[14−16] Their size makes these fibers promising candidates for selected biomedical applications, where their small diameter offers a suitable mimic of collagen fibrils in the natural extracellular matrix, while the corresponding high specific surface area may be advantageous for surface reaction and diffusion processes such as those involved in drug delivery.[17] In most prior studies, caustic solvents (e.g., formic acid and hexafluoro-2-propanol) were used to ensure adequate concentration of the silk fibroin in solution to achieve electrospinnability. After spinning, the silk molecules within the fibers were in the less stable "random coil" and/or helical "silk I" forms,[14,15,18] so that an organic solvent like methanol was required to convert these silk morphologies to the more stable antiparallel β-sheet crystallites (silk II) in the fiber. However, the use of caustic and organic solvents potentially compromises the biocompatibility and mechanical properties of silk fibers.[19] Kaplan and co-workers reported a method for dissolving silk fibroin into aqueous solution up to 8 wt %,[20] and these solutions were subsequently blended with aqueous solutions of PEO to produce spinnable compositions.[20] These solutions were electrospun to produce silk/PEO blended fibers with diameters about 800 nm. Methanol was also used to induce the morphology conversion from random coil and/or silk I in the as-electrospun silk fibers to silk II, but the silk fiber obtained after water extraction was porous.[20,21] In this paper, we report in detail an environmentally benign, entirely aqueous process utilizing a two-fluid electrospinning technique[22] to produce solid, crystallized silk fibers with diameters that are much smaller than natural silk fibers. A schematic of the process is provided in Figure 1. An annealing technique using high humidity was developed to crystallize silk fibers after electrospinning. To our knowledge, this is the first report of conversion of silk fibers from random coil/silk I to silk II using high humidity.

Experimental Method

Materials. Cocoons of *B. mori* silkworm silk were kindly supplied by M. Tsukada, Institute of Sericulture, Tsukuba, Japan. Poly(ethylene oxide) (PEO) (GPC: $M_w = 920\,000$, PDI = 2) was obtained from Scientific Polymer Product Co.

Solution Preparation. The 8 wt % *B. mori* silk solution was prepared as described previously.[19−21]In some instances, 0.1 g/L fluorescein sodium salt (Sigma-Aldrich) was added to the silk solution to facilitate visual observation during electrospinning under UV fluorescent light. In other instances, 0.2 g/L of 7.5 nm diameter Fe_3O_4 particles was added to enhance the contrast of silk fibers in TEM imaging. A 2 wt % PEO solution was prepared under gentle stirring for at least 24 h at room temperature in order to obtain a homogeneous solution. A blended solution containing 16:1 silk: PEO by weight was also prepared by adding the 8 wt % silk solution to the 2 wt % PEO solution at a volume ratio of 4 to 1.

Two-Fluid Electrospinning. The two-fluid electrospinneret, which allows coaxial extrusion of two fluids simultaneously, is shown in Figure 2. The electrospinneret consists of two stainless

[†] Massachusetts Institute of Technology.
[‡] Tufts University.
* Corresponding author: e-mail rutledge@mit.edu.

10.1021/ma0517749 CCC: $33.50
Published on Web 01/11/2006

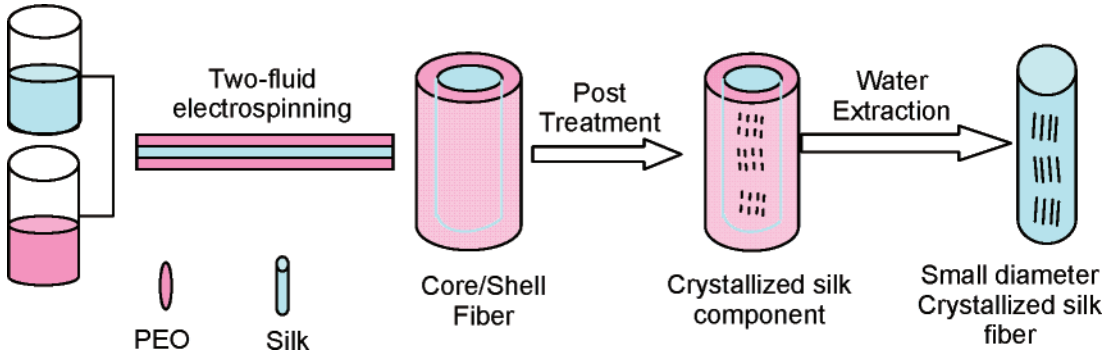

Figure 1. Schematic illustration of the process of producing silk fibers.

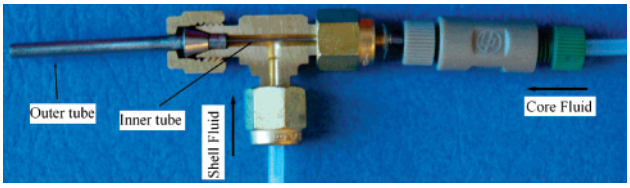

Figure 2. A photo of two-fluid electrospinneret.

steel concentric tubes by which the core (silk) and shell (PEO) fluids are introduced to the spinneret. The inner tube has an inner diameter of 0.45 mm and an outer diameter of 0.80 mm, while the outer tube has an inner diameter of 2.00 mm and an outer diameter of 3.20 mm. The electrospinneret was designed to keep the fluids separate before exiting the nozzle. Similar designs have been reported independently by Sun et al., Li and Xia, Loscertales et al., and Zhang et al.[23−26]

A parallel-plate electrospinning setup was used, similar to that described by Shin et al.[27] Briefly, two aluminum disks with diameters of 12 cm were arranged parallel at a distance of up to 50 cm apart. Two syringe pumps (Harvard Apparatus PHD 4400) were used to deliver the core and shell fluids to the spinneret independently at constant flow rates. The spinneret protruded through the center of the upper disk to a length of 1 cm. An electrical potential was applied to the upper disk by a high-voltage power supply (Gamma High Voltage Research ES-30P). The electrical voltage, flow rates of both core and shell fluids, and distance between the two parallel plates were adjusted to obtain a stable jet. Both the inner and outer tubes were charged to the same electrical potential.

Posttreatment of Electrospun Mats. Electrospun nonwoven mats of silk/PEO fibers were stored ("annealed") in a high relative humidity (RH) chamber (RH 90% at 25 °C) for over 72 h and then washed with water for at least 5 days at room temperature to remove PEO from the mats. For comparison, a thin film was cast from 8 wt % aqueous silk solution at room temperature and annealed at RH 90% under the same conditions. The thickness of the solution-cast silk film is about 10 μm.

Characterization. Images of electrospun fibers were obtained by scanning electron microscopy (JEOL SEM 6320). Infrared spectra were measured with a Nexus 870 spectrophotometer (Thermo Nicolet Corp., UK). Each spectrum was acquired in transmittance mode by accumulation of 128 scans, with a resolution of 4 cm^{-1}. Wide-angle X-ray diffraction (WAXD) data were obtained using a diffractometer (Bruker) with Cu Kα radiation at 40 kV and 20 mA. Transmission electron microscopy (JEOL 200CX) was used to observe the core−shell structure of the fibers. Water content in the as-electrospun silk/PEO fibers was obtained by weighing the fiber before and after heating the fiber at 85 °C for at least 3 days until no obvious weight change was observed with time. Water absorption by electrospun silk/PEO fiber was obtained by weighing the fiber before and after annealing at high RH. Extensional rheological measurements were performed on a HAAKE CABER 1 rheometer (Thermo Electron Corp., Madison, WI). Hencky strain, ϵ, and apparent extensional viscosity, $\bar{\eta}(\epsilon)$, were calculated from the data of evolution of midpoint filament diameter, $D_{mid}(t)$, with time, t.[28−31]

Infrared dichroism was used to measure molecular orientation in the fibers.[32−34] The dichroic ratio D for a particular absorption band is defined by

$$D = A_{\parallel}/A_{\perp} \tag{1}$$

where $A_{\parallel}$ and $A_{\perp}$ represent the peak absorption of infrared radiation polarized parallel and perpendicular, respectively, to the fiber direction. The dichroic ratio can be related to an orientation function, f, through eq 2:

$$f = [(D_0 + 2)/(D_0 - 1)][(D - 1)/(D + 2)] \tag{2}$$

where $D_0 = 2\cot^2\psi$ is the dichroic ratio for perfect alignment and ψ is the angle between the transition moment vector for the vibration and the local chain axis. The orientation function, f, is related to the second moment of molecular orientation $\langle\cos^2\theta\rangle$ by the expression

$$f = [3\langle\cos^2\theta\rangle - 1]/2 \tag{3}$$

$f = 1$ corresponds to perfect uniaxial alignment of molecules in the fiber direction, $f = 0$ corresponds to the absence of preferred orientation, and $f = -1/2$ corresponds to alignment in the plane transverse to the fiber direction. Implicit in the use of this orientation function is the assumption that the uniaxial model is sufficient to represent the state of orientation in these fibers.

Results and Discussion

Extensional Rheology. Extensional rheology was used to characterize the electrospinnability of the aqueous solutions. In a preliminary report of two-fluid electrospinning of core/shell silk/PEO fibers made previously,[22] it was argued that the elasticity of the shell fluid and the low interfacial tension between the two aqueous solutions stabilizes the core fluid against breaking up into droplets by Rayleigh instability. Figure 3a shows the time evolution of the midpoint diameter of the fluid filament for the 8 wt % silk solution, 2 wt % PEO solution, and the 16:1 silk/PEO blend solution. The filament of silk fluid decreased in diameter very fast and broke up in 0.04 s. The filament of PEO fluid decreased in diameter more slowly and broke at 0.60 s. The silk/PEO blend behaved like the silk solution at short times (<0.05 s) but without breaking; at long times, it exhibited the elasticity characteristic of the PEO solution. The silk/PEO filament broke at 0.55 s. This is reflected also in the apparent extensional viscosity vs Hencky strain, shown in Figure 3b. The silk solution behaves like a low-viscosity Newtonian fluid and, on its own, electrosprays. Strain hardening is seen for both PEO and silk/PEO blend solutions. This strain hardening effect is an attribute of the PEO elasticity

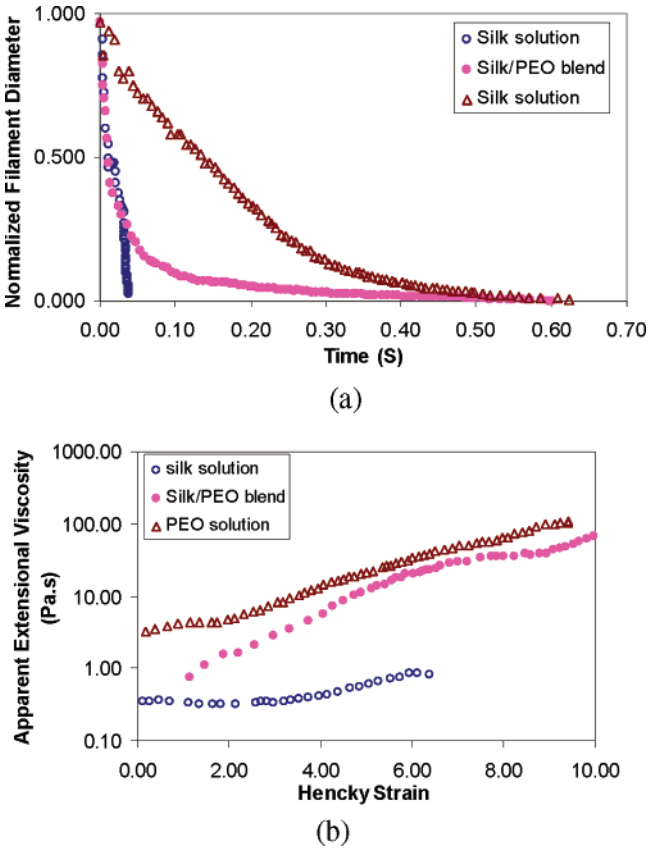

Figure 3. (a) Evolution of filament midpoint diameter vs time for the silk solution, PEO solution, and solution of silk/PEO blend. (b) Apparent extensional viscosity vs Hencky strain for the corresponding materials.

and helps to suppress the breakup of the jet into droplets during the electrospinning.[35,36]

Two-Fluid Electrospinning. To explore the influence of processing parameters, such as flow rates, on the fiber morphology, several combinations of outer (shell) and inner (core) fluid flow rates were tested, ranging from 0.01 to 0.05 mL/min for outer fluid flow rates and from 0.001 to 0.008 mL/min for inner fluid flow rates. The detailed results are summarized in Table 1. As shown in Table 1, the outer diameter of the fibers increased with outer fluid flow rate and the inner diameter of the fiber increased with inner fluid flow rate. However, the shell diameter changed only minutely when the inner fluid (silk) flow rate was increased 5-fold. The entrainment of the silk solution becomes problematic when its flow rate is either too fast or too slow. If it is too slow, there is not enough solution to supply to the core

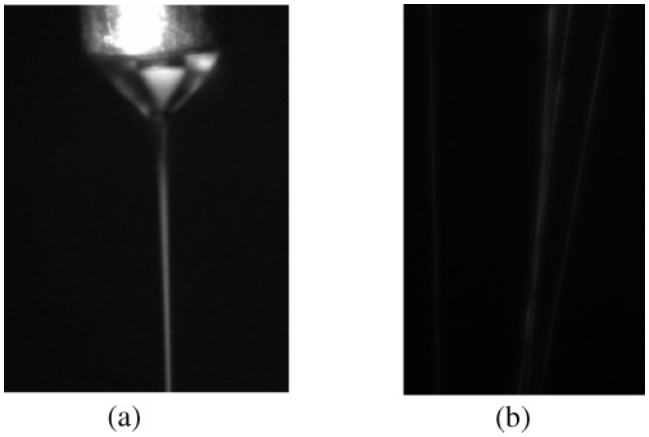

Figure 4. (a) Coaxial PEO and silk fluid jets formed during two-fluid electrospinning in the fluorescent light. (b) Fluorescent image of as-electrospun *B. mori* silk/PEO fibers. (Note: a fluorescent dye was added into the silk solutions before electrospinning.)

of the fiber. As a result, no continuous silk fiber is obtained after extraction. As the silk solution flow rate increases, a nonuniform silk core fiber starts to form. A further increase in the inner fluid flow rate leads to the formation of a uniform core fiber. On the other extreme, when the inner fluid flow rate is too high, the silk solution is no longer entrained within the PEO (shell) solution, causing spraying to occur. To obtain a uniform, continuous core/shell fiber, the ratio of outer and inner flow rates should be in the range of 6:1−10:1, which is a little larger than the exit area ratio of the outer and inner tubes (5:1). Within this range of flow rate ratios, the ratio of the cross-sectional area of the outer fiber to that of the inner fiber increases linearly with the flow rate ratio.

Figure 4a shows a coaxial jet of silk and PEO solutions as the two fluids exit the spinneret under fluorescent light. A fluorescent dye was added to the core silk fluid to facilitate experimental observation. A well-formed silk cone is clearly visible within the PEO cone as the fluids exit the nozzle. The sharp boundary between the two fluids indicates that no significant phase mixing takes place near the nozzle. During the electrospinning process, after ejecting from the apex of the Taylor cone, the charged liquid jet experiences a whipping instability in air before hitting the grounded collecting device. The short travel time of the jet in the air, typically on the order of milliseconds, is far shorter than the time needed for significant diffusional spreading.[23,24] Therefore, significant mixing between the two fluids during the two-fluid electrospinning is unlikely. Continuity of the silk component in the solid fibers was verified

Table 1. Summery of Fiber Diameters: Top Value Is the Outer Fiber Diameter, Bottom Value Is the Inner Fiber Diameter, and Value in Parentheses Is the Standard Deviation

	outer flow rate (mL/min)			
inner flow rate (mL/min)	0.02	0.03	0.04	0.05
0.001	650 nm (s.d. 40) no fiber	690 nm (s.d. 30) no fiber	750 nm (s.d. 30) no fiber	800 nm (s.d 50) no fiber
0.002	660 nm (s.d. 80) nonuniform fiber	680 nm (s.d. 30) 170 nm (s.d. 40)	740 nm (s.d 60) no fiber	810 nm (s.d. 30) no fiber
0.003	nonuniform fiber nonuniform fiber	690 nm (s.d. 40) 250 nm (s.d. 50)	750 nm (s.d. 70) no fiber	800 nm (s.d 50) no fiber
0.004	spray	690 nm (s.d. 50) 360 nm (s.d. 70)	780 nm (s.d. 60) 260 nm (s.d 60)	820 nm (s.d. 50) no fiber
0.005	spray	710 nm (s.d. 70) 480 nm (s.d 80)	760 nm (s.d. 60) 560 nm (s.d. 90)	790 nm (s.d. 70) no fiber
0.006	spray	spray	750 nm (s.d. 70) 650 nm (s.d. 70)	790 nm (s.d. 80) 620 nm (s.d. 90)
0.007	spray	spray	780 nm (s.d. 60) nonuniform fiber	770 nm (s.d. 90) 660 nm (s.d. 90)

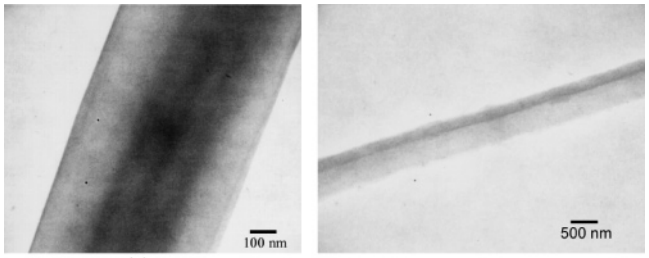

Figure 5. TEM images of as-electrospun *B. mori* silk/PEO fibers: (a) core/shell strecture; (b) side-by-side structure. (Note: 7.5 nm iron oxide nanoparticles were added into the silk solutions before electrospinning.)

by fluorescent imaging of the as-electrospun product (Figure 4b). Imaging by TEM of the as-electrospun silk/PEO fibers (using iron oxide nanoparticles in the silk solution for contrast) also confirms the lack of significant mixing between the two fluids during formation of the fibers (Figure 5). The core/shell structure of the silk/PEO fiber was further characterized by TEM images. Most fibers show the core/shell structure, with silk as core and PEO as shell (Figure 5a). In rare cases, the silk core is off axis in the fiber (Figure 5b).

Posttreatment of Electrospun Mats. Figure 6 shows a series of SEM images of electrospun silk/PEO (core/shell) fibers at various processing stages. During the course of this study, it was discovered that simply storing the as-electrospun fibers, as shown in Figure 6a, under high humidity (overnight at RH 90% at 25 °C) was sufficient to induce the conformation transition of silk fibroin from the less stable random coil and/or silk I form to predominantly the more stable silk II (β sheet) form. Superficially, the resulting fibers appear to be slightly swollen, but otherwise physically unaltered (Figure 6b). However, subsequent extraction with water shows that the silk had become insoluble. After removal of the PEO shell, continuous, uniform silk fibers were obtained (Figure 6c).

The presence of silk II in the final fibers was confirmed by FTIR spectroscopy and X-ray diffraction. In Figure 7, before annealing, the silk fibers showed a peak at 1660 cm^{-1}, characteristic of the random coil and/or silk I conformation.[37,38] It is difficult to distinguish the random coil from silk I conformation in the IR spectrum.[39,40] It is common for these forms to coexist, and both are relatively less stable than the silk II structure, so we have not attempted to distinguish them in the present analysis. After annealing, a new peak appeared at 1630 cm^{-1}, which is characteristic for silk II (β sheet).[37,38] The 1660 cm^{-1} peak was observed to decrease dramatically, while the 1630 cm^{-1} increased dramatically over an initial period of 72 h. After 72 h, the intensities of both peaks changed very slowly. Figure 8 compares the wide-angle X-ray diffraction spectra for degummed native silk fibers with the silk/PEO fibers after humidity treatment and water extraction. Three peaks at $2\theta = 8.5°$, 20.4°, and 24.6°, which are characteristic peaks of β-sheet crystallite, are observed for both fibers.[9,19] It is well-known that the transformation of silk from random coil/silk I to silk II can be induced immediately after immersion in organic solvents such as methanol.[37−41] It is believed that methanol disrupts the hydrogen bonds and permits swelling of the silk so that the polymer chains move more freely to form β sheets.[40−42] We speculate that the same mechanism occurs at high humidity, mediated by the water vapor. The rapid evaporation of solvent from the silk fibers during the electrospinning process reduces the water content of the final fibers to about 7 wt %. After 24 h at 25 °C and RH 90%, the water content of the fibers increased to 20 wt %. The absorbed water could break the hydrogen bond between the silk molecules and swell the silk filaments just as organic solvents do, thereby facilitating transformation. The progressive increment of silk II components using high humidity would make it possible for us to control the degree of crystallinity in the silk fibers through choice of annealing protocols for different applications.

A solution-cast silk film (~10 μm) was also annealed at the RH 90% over 72 h. It was found that only silk fibroin at the surface of the film (~1 μm deep) was converted from random coil and/or silk I to silk II structure, which was confirmed by ATR−IR (not shown); silk at the core of the film remained in the random coil and/or silk I structure, which was also confirmed by the FT-IR and WAXD (not shown). These are consistent with the results obtained by Kaplan et al., who annealed a thick solution-cast pure silk film (~130 μm) under high humidity (more than RH 100%) for 24 h.[43,44] That work indicated that the humidity-induced morphology conversion starts from the surface of the silk film and that the crystallized silk layer which forms initially at the surface of the film might prevent vapor from subsequently accessing silk fibroin at the core of the film. Since this layer is apparently about 1 μm thick, the submicron length scale of the PEO/silk fibers reported here is therefore necessary for the conversion of silk fibroins from random coil and/or silk I to predominantly silk II structure and makes the possibility of converting to silk II by humidity a practical consideration. The benign processing condition realized here also creates a unique opportunity to process labile molecules into these fibers (e.g., other proteins, drugs, growth factors, etc.) and thereby allows the use of such chemistries to create functional materials and delivery systems.

The presence of molecular orientation in the fibers, induced by electrospinning, could also facilitate the transformation to silk II. To test this, we used polarized IR spectroscopy on a unidirectionally oriented mat of electrospun silk/PEO fibers, prepared as described by Li et al.[45,46] The results are shown in Figure 9. The peak at 1342 cm^{-1} is due to the $-CH_2$ wagging vibration of PEO, whose transition moment is parallel to the main chain direction ($\psi = 0°$).[47,48] The peak at 1660 cm^{-1} is

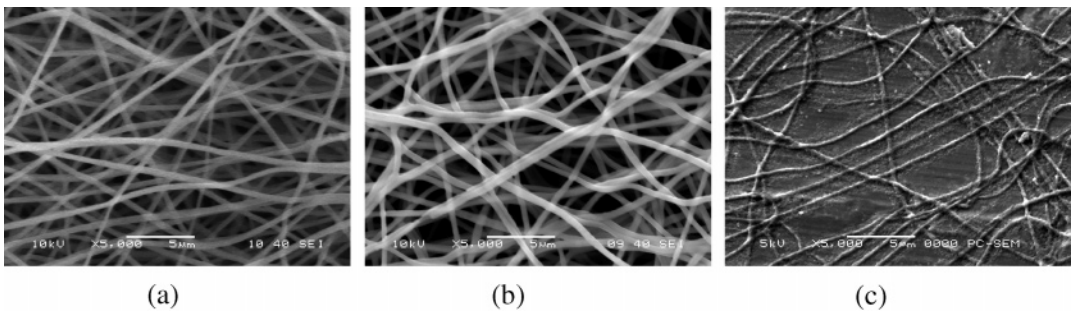

Figure 6. SEM images of *B. mori* silk/PEO fibers ($Q_{outer} = 0.03$ mL/min, $Q_{inner} = 0.003$ mL/min): (a) as-electrospun fibers, (b) electrospun fibers after annealing at RH 90% for 24 h, (c) electrospun fibers after annealing and extraction with water.

Table 2. FT-IR Absorbance, Dichroic Ratio, and Orientation Function for Electrospun Silk/PEO Fibers (Oriented and Isotropic) and Solution-Cast Silk Film

		dichroic ratio	orientation function
unidirectionlly oriented silk/PEO mat	at 1656 cm^{-1}	0.923 ± 0.018	0.053 ± 0.012
	at 1342 cm^{-1}	1.300 ± 0.016	0.092 ± 0.005
unoriented silk/PEO mat	at 1656 cm^{-1}	1.020 ± 0.002	0.010 ± 0.001
	at 1342 cm^{-1}	1.063 ± 0.004	0.021 ± 0.003
solution-cast silk film	at 1656 cm^{-1}	1.042 ± 0.002	0.010 ± 0.002

due to the amide carbonyl stretching (amide I) of silk, whose transition moment is perpendicular to the main chain direction ($\psi = 90°$).[37] The absorbance at 1342 cm^{-1} was higher for parallel polarization than perpendicular; the opposite was true at 1660 cm^{-1} (Figure 9). This indicates that both the PEO and silk components are preferentially oriented along the fiber direction as a result of electrospinning. The measured dichroic ratio and the resulting orientation function are reported in Table 2, along with data for an unoriented electrospun fiber mat and a cast silk film. Though small, the orientation parameters for the oriented fibers are significantly higher than for the unoriented samples and cast silk film. It is worth noting that the orientation of the fibers in the oriented mat was not perfect, so what we measured was a conservative value of molecular orientation in the electrospun silk/PEO fibers.

Conclusions

Submicron diameter silk/PEO fibers with core/shell structure were produced by a two-fluid electrospinning technique at ambient conditions using water as the common solvent. From the extensional rheology, the silk solution behaves like a Newtonian fluid while strong strain hardening was observed for the PEO solution. The two-fluid electrospinning process is the key to produce a continuous core filament of unblended silk. No significant mixing between the two fluids was observed to occur during electrospinning. By adjusting the inner or outer flow rates, silk/PEO fibers with a range of shell/core fiber diameters could be obtained.

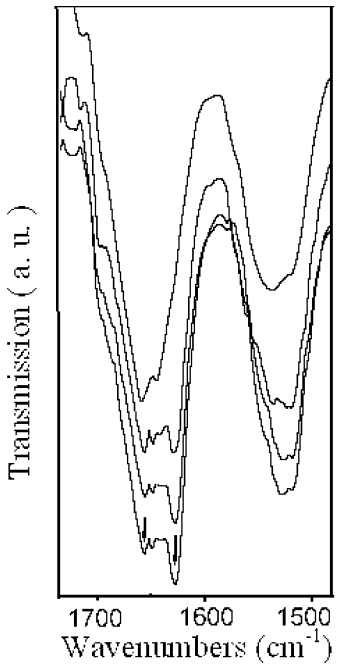

Figure 7. FT-IR spectra of as-electrospun silk/PEO fibers in the amide I region after humidity annealing at RH 90% for different times (Note: from top to bottom, before annealing, 24 h, 48 h, and 72 h annealing, respectively, curves are shifted vertically for clarity. Two peaks at 1660 and 1630 cm^{-1}, which are characteristic for random coil and/or silk I and silk II, respectively, are indicated by arrows.)

Annealing at high humidity was developed to induce the conformation transformation of silk fibroins in the silk/PEO fibers from the random coil and/or silk I to predominantly the β-sheet structure, which was confirmed by both FTIR and WAXD. The small diameter and modest molecular orientation induced by electrospinning in the silk component of silk/PEO fibers facilitate the conformation transformation. The crystallinity of silk fibers could be easily tailored through the choice of annealing protocols for various applications. After water

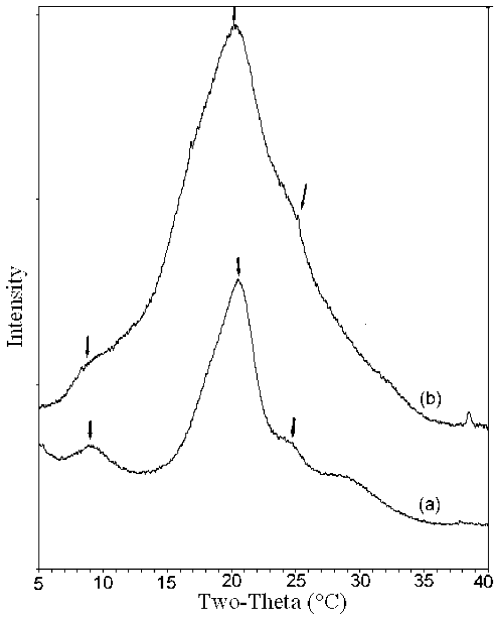

Figure 8. Wide-angle X-ray diffraction spectra: (a) degummed native silk fibers; (b) electrospun silk/PEO fibers after annealing at high humidity and water extraction. (Three peaks at $2\theta = 8.5°$, 20.4°, and 24.6°, designated by arrows, are characteristic peaks of β-sheet crystalline silk II structure.)

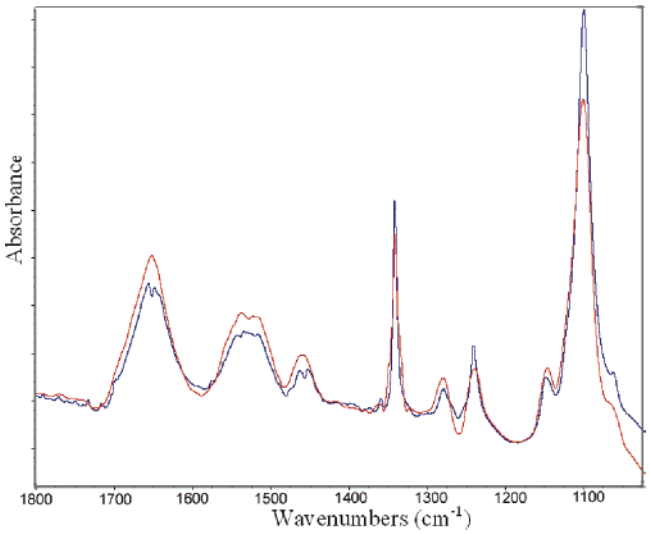

Figure 9. Polarized FT-IR spectra of oriented as-electrospun silk/PEO mat: blue, polarized radiation parallel to the fiber direction; red, polarized radiation perpendicular to the fiber direction.

extraction, a solid, crystallized silk fiber with diameter as small as 170 nm was obtained. As a result, an environmentally benign, entirely aqueous process was developed to produce solid, crystallized silk fibers with diameters that are much smaller than natural silk fibers.

Acknowledgment. We thank Dr. Ung-Jin Kim and Dr. Akira Matsumoto for providing the silk solutions for this study and Dr. Sergey Fridrikh for valuable discussion on extensional rheology of polymer solutions. This research was supported by the U.S. Army through the Institute for Soldier Nanotechnologies, under Contract DAAD-19-02-D0002 with the U.S. Army Research Office.

References and Notes

(1) Kaplan, D. L.; Adams, W. W.; Farmer, B.; Viney, C. In *Silk Polymers: Materials Science and Biotechnology*; *ACS Symp. Ser.* **1994**, *544*.
(2) Vollrath, F.; Knight, D. P. *Nature (London)* **2001**, *410*, 541.
(3) Jin, H. J.; Kaplan, D. L. *Nature (London)* **2003**, *424*, 1057.
(4) Santin, M.; Motta, A.; Freddi, G.; Cannas, M. *J. Biomed. Mater. Res.* **1999**, *46*, 382.
(5) Hudson, S. M. In *Protein-Based Materials*; McGrath, K., Kaplan, D. L., Eds.; Birkhauser: Boston, MA, 1997; pp 311−313.
(6) Kaplan, D. L.; Mello, C. M.; Arcidiacono, S.; Fossey, S.; Senecal, K.; Muller, W. In *Protein-Based Materials*; McGrath, K., Kaplan, D. L., Eds.; Birkhauser: Boston, MA, 1997; pp 313−317.
(7) Lock, R. L. U.S. Patent 5,252,285, 1993.
(8) Fahnestock, S. R. Int. Application # PCT/US94/06689, Int. Publication # WO 94/29450, 1994.
(9) Trabbic, K. A.; Yager, P. *Macromolecules* **1998**, *31*, 462.
(10) Yao, J.; Masuda, H.; Zhao, C. H.; Asakura, T. *Macromolecules* **2002**, *35*, 6.
(11) Seidel, A.; Liivak, O.; Jelinski, L. W. *Macromolecules* **1998**, *31*, 6733.
(12) Liivak, O.; Blye, A.; Shah, N.; Jelinski, L. W. *Macromolecules* **1998**, *31*, 2947.
(13) Seidel, A.; Liivak, O.; Calve, S.; Adaska, J.; Ji, G.; Yang, Z.; Grubb, D.; Zax, D. B.; Jelinski, L. W. *Macrommolecules* **2000**, *33*, 775.
(14) Zarkoob, S.; Eby, R. K.; Reneker, D. H.; Hudson, S. D.; Ertley, D.; Adams, W. W. *Polymer* **2004**, *45*, 3973.
(15) Ohgo, K.; Zhao, C. H.; Kobayashi, M.; Asakura, T. *Polymer* **2003**, *44*, 841.
(16) Sukigara, S.; Gandhi, M.; Ayutsede, J.; Micklus, M.; Ko, F. *Polymer* **2003**, *44*, 5721.
(17) Zong, X.; Kim, K.; Fang, D.; Ran, S.; Hsiao, B. S.; Chu, B. *Polymer* **2002**, *43*, 4403.
(18) Stephens, J. S.; Fahnestock, S. R.; Farmer, R. S.; Kiick, K. L.; Chase, D. B.; Rabolt, J. F. *Biomacromolecules* **2005**, *6*, 1405.
(19) Min, B. M.; Lee, G.; Kim, S. H.; Lee, T. S.; Park, W. H. *Biomaterials* **2004**, *25*, 1289.
(20) Jin, H. J.; Fridrikh, S. V.; Rutledge, G. C.; Kaplan, D. L. *Biomacromolecules* **2002**, *3*, 1233.
(21) Wang, M.; Jin, H. J.; Kaplan, D. L.; Rutledge, G. C. *Macromolecules* **2004**, *37*, 6856.
(22) Yu, J. H.; Fridrikh, S. V.; Rutledge, G. C. *Adv. Mater.* **2004**, *16*, 1562.
(23) Sun, Z.; Zussman, E.; Yarin, A. L.; Wendorff, J. H.; Greiner, A. *Adv. Mater.* **2003**, *15*, 1929.
(24) Li, D.; Xia, Y. *Nano Lett.* **2004**, *4*, 933.
(25) Loscertales, I. G.; Barrero, A.; Guerrero, I.; Cortijo, R.; Marquez, M.; Ganan-Calvo, A. M. *Science* **2002**, *295*, 1695.
(26) Zhang, Y. Z.; Huang, Z. M.; Xu, X. J.; Lim, C. T.; Ramakrishna, S. *Chem. Mater.* **2004**, *16*, 3406.
(27) Shin, Y. M.; Hohman, M. M.; Brenner, M. P.; Rutledge, G. C. *Polymer* **2001**, *42*, 9955.
(28) Anna, S. L.; McKinley, G. H. *J. Rheol.* **2001**, *45*, 115.
(29) McKinley, G. H.; Brauner, O.; Yao, M.; Proc. 1st International Symposium on Applied Rheology, Korea, Jan 18−19, 2001.
(30) Kolte, M.; Szabo, P. *J. Rheol.* **1999**, *43*, 609.
(31) Spiegelberg, S.; Ables, D.; McKinley, G. *J. Non-Newtonian Fluid Mech.* **1996**, *64*, 229.
(32) Pedicini, A.; Farris, R. J. *Polymer* **2003**, *44*, 6857.
(33) Estes, G. M.; Seymour, R. W.; Cooper, S. L. *Macromolecules* **1971**, *4*, 452.
(34) Seymour, R. W.; Allegrezza, A. E.; Cooper, S. L. *Macromolecules* **1973**, *6*, 896.
(35) Wang, M.; Hsieh, A. J.; Rutledge, G. C. *Polym. Mater. Sci. Eng.* **2004**, *91*, 818.
(36) Wang, M.; Hsieh, A. J.; Rutledge, G. C. *Polymer* **2005**, *46*, 3407.
(37) Hallmark, V.; Rabolt, J. F. *Macromolecules* **1989**, *22*, 500.
(38) Ishida, M.; Asakura, T.; Yokoi, M.; Saito, H. *Macromolecules* **1990**, *23*, 88.
(39) Asakura, T.; Kuzuhara, A.; Tabeta, R.; Saito, H. *Macromolecules* **1985**, *18*, 1841.
(40) Chen, X.; Shao, Z. Z.; Marinkovic, N. S.; Miller, L. M.; Zhou, P.; Chance, M. R. *Biophys. Chem.* **2001**, *89*, 25.
(41) Tsukada, M.; Gotoh, Y.; Nagura, M.; Minoura, N.; Kasai, N.; Freddi, G. *J. Polym. Sci., Part B: Polym. Phys.* **1994**, *32*, 961.
(42) Spek, E. J.; Wu, H. C.; Kallenbach, N. R. *J. Am. Chem. Soc.* **1997**, *119*, 5053.
(43) Park, J.; Kaplan, D. L. Master Thesis, Tufts University, 2004.
(44) Jin, H. J.; Park, J.; Karageorgiou, V.; Kim, U.; Valluzzi, R.; Cebe, P.; Kaplan, D. L. *Adv. Funct. Mater.* **2005**, *15*, 1241.
(45) Li, D.; Herricks, T.; Xia, Y. *Appl. Phys. Lett.* **2003**, *83*, 4586.
(46) Li, D.; Wang, Y.; Xia, Y. *Adv. Mater.* **2004**, *16*, 361.
(47) Enriquez, E. P.; Granick, S. *Colloids Surf., A* **1996**, *113*, 11.
(48) Hoffmann, C. L.; Rabolt, J. F. *Macromolecules* **1996**, *29*, 2543.

MA0517749